



Published in final edited form as:

NMR Biomed. 2012 September ; 25(9): 1104–1111. doi:10.1002/nbm.2776.

Early prediction of response to Vorinostat in an orthotopic glioma rat model

Li Wei^{1,§}, Samuel Hong^{2,§}, Younghyun Yoon², Scott N. Hwang², Jaekeun C. Park¹, Zhaobin Zhang³, Jeffrey J. Olson³, Xiaoping P. Hu¹, and Hyunsuk Shim^{2,4,*}

¹Department of Biomedical Engineering, Emory University, Atlanta, Georgia 30322, USA.

²Department of Radiology and Imaging Sciences, Emory University, Atlanta, Georgia 30322, USA.

³Department of Neurosurgery, Emory University, Atlanta, Georgia 30322, USA.

⁴Winship Cancer Institute, Emory University, Atlanta, Georgia 30322, USA.

Abstract

Glioblastoma (GBM) is the most common primary brain tumor and is uniformly fatal despite aggressive surgical and adjuvant therapy. Since survival is short, it is critical to determine the value of therapy early on in treatment. Improved early predictive assessment would allow neuro-oncologists to personalize and adjust or change treatment sooner to maximize use of efficacious therapy. During carcinogenesis, tumor suppressor genes can be silenced by aberrant histone deacetylation. This epigenetic modification has become an important target for tumor therapy. Suberoylanilide hydroxamic acid (SAHA, Vorinostat, Zolinza; Merck & Co., Inc.) is an orally active, potent inhibitor of histone deacetylase (HDAC) activity. A major shortcoming of the use of HDAC inhibitors in treating brain tumor patients is the lack of reliable biomarkers to predict and determine response. Histological evaluation may reflect tumor viability following treatment but it is an invasive procedure and impractical for GBM. Another problem is that response to SAHA therapy is associated with tumor redifferentiation and cytostasis rather than tumor size reduction, thus limiting the use of traditional imaging methods. A noninvasive method to assess drug delivery and efficacy is needed. Here, we investigated whether changes in ¹H MRS metabolites could render reliable biomarkers for an early response to SAHA treatment in an orthotopic animal model for glioma. Untreated tumors exhibited significantly elevated alanine and lactate levels and reduced inositol, NAA and creatine, typical changes reported in GBM compared to normal brain tissues. The proton MRS-detectable metabolites of SAHA treated tumors were restored toward those of normal-like brain tissues. In addition, reduced inositol and NAA were found to be potential biomarkers for mood alteration and depression, which may also be alleviated with SAHA treatment. Our study suggests that ¹H MRS can provide reliable metabolic biomarkers at the earliest stage of SAHA treatment to predict the therapeutic response.

Keywords

MRS; histone deacetylase inhibitor; glioma; SAHA; vorinostat; myo-inositol; orthotopic; depression

* Correspondence to: H. Shim, Department of Radiology and Imaging Sciences, Winship Cancer Institute, Emory University, 1701 Uppergate Drive, C5018, Atlanta, GA 30322, Tel: 404-778-4564, Fax: 404-712-5813, hshim@emory.edu.

§These authors contributed equally to this work.

INTRODUCTION

Glioblastoma (GBM) is the most common and aggressive type of primary brain tumor in humans. GBMs involve glial cells and account for 52% of all parenchymal brain tumors and 20% of all intracranial tumors. Despite multimodality treatments, which consist of open craniotomy with maximal surgical resection of the tumor, followed by concurrent or sequential chemoradiotherapies, anti-angiogenic therapy with bevacizumab, and symptomatic care with corticosteroids, the median survival of GBM patients remains approximately 14 months under best circumstances (1). Current treatment options for GBM patients are limited by both acquired and inherent tumor resistance, which include the blood-brain barrier (BBB) and tumor hypoxia (2,3). During carcinogenesis, tumor-suppressor genes can be silenced by aberrant histone deacetylation through histone deacetylase (HDAC). This epigenetic modification has been recognized with high incidence and has become an important target for anticancer therapy in GBM (4–6).

Histone deacetylation by HDACs is one of the main mechanisms involved in the regulation of gene expression (7). The action of HDACs on nucleosomal histones leads to condensed coiling of chromatin, and thus silencing of the expression of various genes, including those implicated in the regulation of cell survival, proliferation, tumor cell differentiation, cell cycle arrest, and apoptosis (8). HDACs are not limited to involvement in histone deacetylation, but also act as members of protein complexes to prevent recruitment of transcription factors to the promoter region of genes, including tumor suppressors, and affect the acetylation status of specific cell cycle regulatory proteins (9). HDAC-inhibitors (HDACi) can efficiently suppress HDACs' activity and inverse histone deacetylation. In the presence of HDAC-inhibitors, chromatin remains in an open configuration, allowing transcription factors to reach DNA promoters and facilitate the transcription of tumor suppressor genes that check the growth of cancer cells. Over the last 5 years, numerous HDAC-inhibitors have been evaluated in clinical trials (review in (10)). They commonly display the ability to hyperacetylate both histone and non-histone targets, resulting in a variety of effects on cancer cells, their microenvironment, and immune responses.

Vorinostat (Suberoylanilide hydroxamic acid-SAHA, Zolinza™; Merck & Co., Inc., Whitehouse Station, NJ) is an orally active, potent inhibitor of HDAC activity, which was approved by the FDA in 2006 for the treatment of refractory cutaneous T cell lymphoma (11). To date, responses with this single agent HDACi have been predominantly observed in advanced hematologic malignancies including T-cell lymphoma, Hodgkin lymphoma, and myeloid malignancies (12). SAHA mainly inhibits HDAC 1, 2, 3, 6, and 8, selectively up-regulating the expression of pro-apoptotic members of the B-cell lymphoma (Bcl)-2 family and down-regulating the expression of anti-apoptotic genes such as Cyclin-dependent kinase (CDK)2, CDK4, cyclin D1, and cyclin D2 (13). SAHA also increases the expression of tumor necrosis factor (14) and induces the acetylation of the chaperone protein Hsp90 (heat shock protein 90), which leads to cellular stress and apoptotic cell death (15). Furthermore, animal studies have shown that SAHA is capable of crossing the blood brain barrier, as it increases H3 and H4 acetylation in brain tissue (14). SAHA is being evaluated in many types of cancers, including lung, breast, and colon cancers, and it may also be a welcome addition for the treatment of GBM (16–18). The antitumor activity of SAHA against malignant gliomas has been reported (19); however, there are only a small number of reports examining the effects of SAHA treatment on gliomas with non-invasive *in vivo* studies, and few examined the changes in cerebral metabolites in tumors.

In vivo ¹H MRS has been widely used to study brain tumor metabolism in preclinical animal models and in clinical research. It can identify specific genetic and metabolic changes that occur in malignant tumors without introducing exogenous variables. Traditionally, N-

acetylaspartate (NAA) has been used as a marker for neurons, total choline (tCho) as existing in the membrane of cells, creatine (Cr) as involved in the metabolism of energy, inositol (Ins) as a marker for glial cells, and lactate (Lac) and alanine (Ala) as products of anaerobic pathways (20,21). As a result, metabolic markers, detectable by MRS, not only provide information on biochemical changes but also define different metabolic tumor phenotypes.

Ins is a carbocyclic polyol that plays an important role as the structural basis for a number of secondary messengers in eukaryotic cells, including inositol phosphates, phosphatidylinositol (PI) and phosphatidylinositol phosphate (PIP) lipids. Ins is synthesized from glucose-6-phosphate (G-6-P) in two steps. First, G-6-P is isomerised by inositol-3-phosphate synthase (ISYNA1) to inositol-1-phosphate, which is then dephosphorylated by IMPase1 to give free Ins (22,23). It has been reported that the histone deacetylase RPD3 directly regulate ISYNA1 (also known as INO1 or MIP1), and that a mutation in RPD3 can cause a 32-fold increase in ISYNA1 mRNA level (7). Recent studies showed that Ins level was low in the cerebrospinal fluid of patients with depression, and that treating them with Ins could significantly improve their behavioral test scores (24,25). Depressive symptoms are also common behavioral changes in patients with cancer and cancer survivors, and such changes are reported in 30–50% of brain tumor patients (26,27). Taken together, the tumor Ins profile, detectable through MRS and/or molecular biology method, may serve as a promising biomarker for the therapeutic activity of SAHA treatment in malignant glioma.

Given that GBM patient survival time is very short, it is critical to determine the therapeutic activity at the earliest stage of SAHA treatment and to enable oncologists to make timely changes in the treatment of patients for whom therapy failed. In this study, changes in the cerebral metabolites in the orthotopic glioma rat model were measured 3 days after SAHA treatment. The changes were consistent with improved mood-related behaviors and altered gene expression profile. Our main aim of the study was to establish reliable biomarkers at the earliest stage of SAHA treatment to predict the therapeutic response.

MATERIALS AND METHODS

Animal model of gliomas and *in vivo* SAHA administration

9L rat glioma cells (50,000 cells in 5 μ l volume) were stereotactically injected into the brains of male Fischer 344 rats at stereotactic coordinates 1 mm forward of the frontal zero plane, 3 mm to the right of midline, and 4.5 mm deep (28). SAHA was resuspended in 10% polyethylene glycol (PEG)-200 and 90% of 0.5% methylcellulose. The rats bearing intracranial tumor were treated with an intraperitoneal injection of the vehicle (control group, n=5) or SAHA starting from day 9 until day 12 after the initial tumor cell injection. The treated groups received a dose of 25 (n=5), 50 (n=5), or 75 mg/kg/day (n=12) of SAHA. The control group and the group treated with 75 mg/kg/day of SAHA were subjected to MRS scans on day 12. The tumors were collected from all groups to measure ISYNA1 mRNA levels following the MR examinations. All protocols for animal studies were reviewed and approved by the Institutional Animal Care and Use Committee (IACUC) at Emory University.

MR/MRS protocol

All MR data were acquired with a 9.4 T/20 cm horizontal bore Bruker magnet, interfaced to an Avance console (Bruker, Billerica, MA) and equipped with an actively shielded gradient set (an inner diameter of 11.6 cm, maximum gradient strength of 200 mT/m, and 110 μ sec rise time). A two-coil actively decoupled imaging setup was used (a 3 cm diameter surface coil for reception and a 7.2 cm diameter volume coil for transmission) to achieve maximal SNR over the cortical and subcortical areas of interest. Rats were initially anesthetized with

5% isoflurane in O₂, which was reduced to 1.5~2% for maintenance. The head of the rat was secured using foam padding to minimize possible movements. Respiration, electrocardiogram (ECG), and blood oxygen level were monitored and rats were kept normothermic at 37°C using a circulating water blanket. T₂-weighted anatomical reference images were acquired with a multi-slice multi-spin-echo sequence for tumor localization. Imaging parameters were: TE=15, 30, 45, 60, 75 ms; TR= 2500 ms; matrix size 128 × 128; slice thickness 8 mm; 16 slices; FOV 2.5 cm×2.5 cm. After localization, ¹H MR spectra were acquired from the tumor side and contra-lateral side of each rat by using a STEAM (stimulated echo acquisition mode) sequence with the following parameters: TE =20 ms; TR = 4000 ms; TM = 15 ms; 2048 complex data points; spectral bandwidth of 4000 Hz; voxel size 5 mm×5 mm×5 mm; 256 averages. The water signal was suppressed by a VAPOR scheme. The typical linewidth for the water resonance after shimming with FASTMAP was 8–10 Hz. All MR-STEAM spectra data were analyzed by the LC model software (Linear Combination of Model spectra, version 6.2.0), using the water signal as an internal reference and a 23 metabolite basis-set including but not limited to glycerophosphocholine (GPC), choline (Cho), phosphocholine (pCho), creatine (Cr), phosphocreatine (pCr), glutamate (Glu), glutamine (Gln), taurine (Tau), inositol (Ins), glycine (Gly), glucose (Glc), N-acetylaspartate(glutamate) (NAA(G)), alanine (Ala), gamma-aminobutyrate (GABA), aspartate (Asp), glutathione (GSH), lactate (Lac), guanidoacetate (Gua), and scyllo-inositol (sI). Statistical analysis was performed with student *t*-tests.

A frequency-Selective Double quantum coherence (Sel-DQC) method based on PRESS (29,30) was implemented to measure the Ala and Lac peaks separately which overlap the peaks of lipids and macromolecules (Fig. 2a). We used Sel-DQC to selectively detect the methyl protons (–CH₃) of lactate at 1.31 ppm that were coupled with methylene protons (–CH=) of Lac at 4.09 ppm and the methyl protons (–CH₃) of Ala at 1.47 ppm that were coupled with methylene proton (–CH=) of Ala at 3.8 ppm. For selective Ala detection, Sel-DQC was used to selectively detect the methyl protons (–CH₃) of Ala at 1.47 ppm, which were J-coupled with the proton of CH of Ala at 3.77 ppm. The DQC path from the excited protons coupling network of Ala was selected by a gradient combination while suppressing the other coherence paths (g₁:g₂ = 1:2, the duration of g₁ and g₂ were the same). Other parameters were: TR = 4000 ms; TE₁ = TE₂ = 35 ms (TE=70ms); TM = 14 ms; 2048 complex data points; spectral bandwidth = 4000 Hz; voxel size 5 mm×5 mm×5 mm; 512 averages. After acquisition, the time signals were zero-filled to 4096 data points and multiplied with a 3 Hz exponential filter.

Cell culture and *in vitro* SAHA administration

SAHA (NCI/CTEP, Bethesda, MD) was dissolved in dimethyl sulfoxide (DMSO) to obtain a 100 mM stock solution. The rat glioma cell line 9L was maintained in Dulbecco's modified eagle medium (DMEM) (Mediatech, Manassas, MA) supplemented with 10% fetal bovine serum (FBS) and antibiotics at 37°C in 5% CO₂. 9L cells were plated in 100 mm cell culture petri-dishes. Cells were then treated three days following seeding with fresh medium containing SAHA at concentrations of 0, 0.1, 0.3, and 1 μM for 6 hours and were collected to prepare total RNA. The cells were also incubated with 1 μM of SAHA in different incubation time points and were collected to assess ISYNA1 mRNA levels. The incubation time lengths were 0 hour, 2 hours, 4 hours, 6 hours, and 12 hours.

RNA isolation, RT-PCR, and real-time RT-PCR

To measure ISYNA1 mRNA levels, total RNA extracted from *in vitro* and *in vivo* samples was prepared with Trizol reagent (Invitrogen, Carlsbad, CA) according to the manufacturer's instructions. Total RNA was then reverse transcribed into cDNA in a 20 μl reaction volume, which included 0.5 μg RNA, 200 μM dNTPs, 2.5 mM MgCl₂, 10 mM

DTT, 8 units RNase inhibitor, 30 units reverse transcriptase, and 1.25 μ M random hexamers in 1 \times RT buffer. GeneAmp Gold RNA PCR Reagent kit (Applied Biosystems, FosterCity, CA) was used for the reverse transcription. cDNA synthesis was performed at 25°C for 10 min followed by 42°C for 45 min, and heating the samples to 70°C for 10 min stopped the reaction. Then the cDNA was stored at 4°C until usage or immediately used for PCR. For the real-time PCR, SYBR Green quantitative PCR amplifications were performed with a multicolor real-time PCR detection system (Bio-Rad, Hercules, CA). The reactions were performed in a 20 μ l reaction volume containing 10 μ l of 2 \times SYBR Green PCR Master Mix (Applied Biosystems), 0.2 μ M of each forward and reverse primer, and 2 μ l of the cDNA. The amplifications were initiated at 95°C for 10 min followed by 40 cycles of 95°C for 30 s, 54°C for 30 s, and 70°C for 20 s. The primers for *ISYNA1* are 5'-GGAGAGGAGCCAGATCACTG and 5'-CAGCACTAGGTCCAGCATGA, and the primers for β -actin are 5'-GACAGGATGCAGAAGGAGAT and 3'-TGCTTGCTGATCCACATCTG (GenBank access number: NM_001013880).

RESULTS

SAHA restores normal brain tissue-like metabolism in brain tumors

Tumor localization and size measurements were performed on the basis of T₂-weighted images. Figure 1a shows the T₂-weighted images obtained from two representative intracranial tumor-bearing rats. The tumors were typically hyperintense in the T₂-weighted images. After three days of treatment, average tumor size was smaller in the SAHA-treated rats (90.3 \pm 18.7 mm³) than in the untreated rats (119.8 \pm 21.5 mm³).

¹H MR spectra obtained from the tumor side and contra-lateral side of each rat were localized on the basis of the T₂-weighted images. Figure 1b shows the STEAM MRS results obtained from two representative rats (SAHA-treated, red; untreated, black). In contrast to the contra-lateral side, all tumor spectra demonstrated decreased levels of Cr, NAA, and Ins with significantly increased levels of Cho, Lac, and Ala (p<0.05). After three days of treatment, the spectra obtained from tumors of the SAHA-treated rats showed increased levels of NAA, Cr, and Ins, and decreased levels of Ala and Lac in comparison to the untreated animals. The concentrations of each metabolite in the spectra are shown in Figure 2b. A decrease in Ala and Lac levels in the tumor after SAHA treatment was confirmed by the Sel-DQC spectra results (Fig. 2). Metabolite concentrations (mean \pm standard deviation) are summarized in Table 1.

SAHA improves mood-related behaviors in rats

Daily behavioral notes for SAHA-treated and untreated tumor-bearing rats were recorded until the endpoint of each rat. In general, SAHA-treated rats demonstrated increased movement than untreated rats as measured by a marked increase in the number of grooming, swaying, sniffing, and climbing-like behaviors. On the other hand, untreated rats showed a significantly decreased amount of activities in general and exhibited a general lack of response to opening of the cage lid. These observations indicate that SAHA may improve depression-induced behaviors in rats bearing gliomas. Interestingly, the behavioral difference between the treated and untreated groups correlates with the difference in MRS Ins levels between the treated and untreated groups.

SAHA increases tumor *ISYNA1* mRNA level *in vivo*

Implanted tumors from the SAHA-treated group with different doses (25, 50, and 75 mg/kg/day), and the untreated group (vehicle) were collected for real-time RT-PCR analysis immediately after the MRS assessment. Figure 3 shows the relative fold-change of *ISYNA1* mRNA level in tumors from both groups. *ISYNA1* mRNA level showed a dose-dependent

increase in response to the treatment, in which an approximately 5-fold increase in the average mRNA level was induced by 75 mg/kg/day of SAHA treatment. 25 mg/kg/day and 50 mg/kg/day of SAHA treatment produced an approximately 3-fold increase in ISYNA mRNA level. Increased ISYNA mRNA level in SAHA-treated tumors correlates with increased MRS Ins levels seen in tumors of the treated group.

SAHA increases 9L ISYNA1 mRNA level *in vitro*

To assess the effect of SAHA on ISYNA1 mRNA levels *in vitro*, 9L cells grown in complete medium were exposed to four different concentrations of SAHA for 6 hours. Figure 4a shows the RT-PCR results of the ISYNA1 mRNA level in cells treated with various concentrations of SAHA. The ISYNA mRNA levels increased in a dose-dependent manner up to 1 μ M.

The 9L rat glioma cell line was also treated with 1 μ M of SAHA in different incubation time lengths. Figure 4b shows the relative fold-change of ISYNA mRNA level in 1 μ M-SAHA treated cells incubated for 0, 2, 4, 6, and 12 hours. The fold-change was greatest between 2 and 4 hours post-treatment, reaching an approximately 6-fold increase at hour 4.

DISCUSSION

SAHA, also known as Vorinostat, is an orally active, potent inhibitor of HDAC1, 2, 3, and 6 activities (31). SAHA not only has a direct impact on gene transcription via the inhibition of HDAC function on histone tails but also targets gene transcription by indirect mechanisms via inhibiting HDAC interactions with non-histone proteins. At high concentration, SAHA consequently results in cellular stress and apoptotic cell death (15).

There is a report that SAHA has antitumor activities against malignant glioma cell lines *in vitro* and *ex vivo* (19). Another study reported that intracranial administration of SAHA by using an orthotopic glioma mouse model increased survival time from 22 days to 42 days (32). In this short-term study, histological analysis showed an 80% reduction in tumor volume in the SAHA-treated group. This reduction in tumor volume was associated with a significant increase in the apoptosis rate and a decrease in proliferation and angiogenesis. In another animal study, *in vivo* murine experiments demonstrated that SAHA (10 mg/kg, intravenously (i.v.), or 100 mg/kg, intraperitoneally (i.p.)) could cross the blood-brain barrier as demonstrated by significantly increased levels of acetyl-H3 and acetyl-H4 in the brain tissue (14). Furthermore, SAHA significantly ($P < 0.05$) inhibited the proliferation of GL26 glioma cells growing in the mouse brain and increased their survival. Eyupoglu et al. reported that a single intratumoral injection of SAHA *in vivo* 7 days after orthotopic implantations of glioma cells in syngenic rats doubled their survival time (19). Galanis et al. reported that SAHA was well-tolerated in patients with recurrent GBM, and nine of the 52 patients were progression-free at 6 months after 14 days of SAHA treatment (33). These observations support SAHA as a possible and promising pharmacotherapy for malignant gliomas.

Conventional MR imaging of high grade gliomas characteristically exhibits vasogenic edema and contrast enhancement. High signal intensity is typically displayed in T₂-weighted and FLAIR images, while low intensity is displayed in T₁-weighted images (34). For non-enhancing gliomas, the response to therapy cannot be gauged by MRI alone. A further difficulty is that the response in many cases is associated with tumor stasis, rather than tumor shrinkage (35), limiting the utility of traditional imaging methods. SAHA can modulate numerous genes and proteins involved in cell survival, proliferation, differentiation, and apoptosis, which may be associated with the changes in visible MRS metabolites within tumor, such as NAA, Cr, Ins and Lac etc.

^1H MRS has been an important tool for detecting metabolite levels in many diseases. It is also currently used as a non-invasive means of classifying and grading brain tumors (36,37). Weis et al. reported that the concentration of tCr might be a potential biomarker for grading the malignant gliomas (37). In astrocytomas, several studies have suggested that tCho concentration positively correlates with tumor grade. However, GBMs usually have lower tCho concentrations compared to grade II and III astrocytomas. This observation could be explained by tumor necrosis, which is associated with a decrease in all metabolites and an increase in Lac/Lipids levels (38). The concentration of tCho depends on the balance of tumor prognosis and necrotic core in the tumor (39). Recent investigations suggest that it also may be an effective prognostic tool for monitoring the patient response to a treatment as the technique can localize regions of heterogeneous tumor regression during and/or following a treatment. The treatment response data may, in turn, help to identify those patients who would likely benefit from specific therapies. In a study of 39 patients with malignant gliomas, Li et al. observed that, prior to surgical resection, large volumes of contrast enhancement, high levels of Cho and Lac, and low levels of NAA and Cr were associated with poor prognosis (20). In a study using ^1H MRS to monitor 16 malignant glioma patients treated with tamoxifen, Sanker et al. found that prior to the treatment, responders had higher levels of Cr and NAA compared to non-responders but had lower levels of Lac (40). Levels of Cho did not differ between the two groups. Thus, the association of metabolites with the treatment response also appears to depend on the treatment modality.

The purpose of the current work was to establish reliable metabolic MRS biomarkers at the earliest stage of SAHA treatment to predict the therapeutic response of GBMs. Although the 9L rat orthotopic brain tumor model is not completely analogous to human gliomas since it grows as a well-defined solid mass rather than as an ill-defined infiltrating tumor, it provides a model system in which to develop the concept of SAHA MRS. However, the observations described in the current work must be confirmed in human tumors. In comparison with the contralateral normal-appearing hemisphere, all tumor spectra exhibited lower levels of NAA, tCr, Ins, and Gln/Glu with higher levels of Cho, Lac, and Ala, which is consistent with previous reports in clinical studies of GBMs (38,41). In comparison with MRS of the untreated group, MRS obtained from tumors of the SAHA treated group showed higher levels of NAA, Cr, and Ins with significantly lower levels of Ala and Lac. There were no significant changes in Cho concentration. These observations suggest that there was an improvement in the metabolic profile within the tumors only three days after SAHA treatment.

NAA is an important metabolite mainly stored within neurons, and the intensity of the NAA peak at 2.02 ppm is considered a spectroscopic neuronal marker for intact axons. Normally, NAA has been reported to be dramatically reduced in high grade gliomas (41). The decrease in NAA level is widely interpreted as the loss, dysfunction or displacement of normal neuronal tissues (42). In the current work, NAA concentrations were higher within the tumors of the SAHA-treated rats than in those of the untreated rats. This observation suggests that there are more viable neurons in the tumor as a result of treatment.

The total Cr peak at approximately 3.02 ppm is reduced in malignant gliomas. Several studies found that tCr may be a sensitive biomarker for tumor response to therapies (40,43). Cr is a nitrogenous organic acid that occurs naturally in vertebrates and helps to supply energy to all cells in the body. It is thought to be low in an active tumor due to energy consumed by dividing neoplastic cells. Consequently, the observed increase in concentration of tCr in the tumors of the SAHA-treated rats may indicate a decrease in rapid tumor cellular division.

Lac and Ala are by-products of anaerobic metabolism and are usually elevated in high-grade gliomas due to their constitutive uses of anaerobic pathways as an energy source. In addition, the intratumoral accumulation of Lac is attributed to the impeded clearance of necrotic tissue within gliomas (44). The decrease in the concentrations of Lac in the tumors of SAHA-treated rats may suggest the amelioration of necrosis and energy consumption due to a decrease in tumor cell division.

The most interesting observation in this study is that the tumors of SAHA-treated rats demonstrate a higher concentration of Ins. An increase in the Ins level is usually observed in lower malignant gliomas and is explained by the infiltration or proliferation of active malignant glial cells. In this case, the decrease in NAA may be associated with an increase in Ins (25). Ins can also be used as a biomarker for grading malignant gliomas (24) since it is increased in low-grade astrocytomas but decreased in GBMs. In our study, the visible MRS Ins level in tumor increased significantly after three days of SAHA treatment. Recent studies showed that Ins level was low in the cerebrospinal fluid of patients with depression, and that treating them with Ins could significantly improve their behavioral test scores (24,25). ISYNA1 is the bottleneck enzyme to produce myo-inositol. Previously, ISYNA1 (also known as INO1) was reported to be directly regulated by a histone deacetylase RPD3 (7). Consistent with this previous report, both our *in vivo* and *in vitro* SAHA administration results showed that there was a dose-dependent increase in the level of ISYNA1 mRNA, demonstrating that SAHA could increase Ins production in tumor cells. Thus, the ISYNA1 mRNA level, along with the MRS Ins profile, may be utilized as an independent biomarker obtainable through biopsy. The recovery of NAA and Ins within tumor suggests that SAHA may induce redifferentiation of brain tumors in which the redifferentiated cells regain normal function and thus produce an elevated amount of Ins and NAA (45). The potential redifferentiation effect of SAHA sustained by the restoration of Ins level may also be the underlying etiology of the observed mood-stabilization. Mood-stabilizing actions of HDAC inhibitors have also been recently reported by multi-institutional preclinical studies (46). Ins is a simple isomer of glucose and is a key metabolic precursor in the phosphatidylinositol (PI) cycle. Unlike L-DOPA and tryptophan, which are amino acid precursors of monoamine neurotransmitters and have been reported to have antidepressant properties, Ins is a precursor of an intracellular second messenger system. The PI cycle is a second messenger system for numerous neurotransmitters (47). Barkai et al. reported that depressed patients, both unipolar and bipolar, had markedly reduced levels of Ins in cerebrospinal fluid (CSF) (48). In the study of eleven depressed patients who had been resistant to previous antidepressant treatments, Ins treatment led to a decline in mean Hamilton Depression Scale from 31.766 to 16.269. They showed that 12 g daily intake of Ins raised CSF Ins levels by 70% (49). Levine et al. in his review article, made a comparison of eight controlled studies of Ins treatment in different psychiatric disorders and suggested that Ins had therapeutic effects in the spectrum of illnesses responsive to serotonin-selective re-uptake inhibitors, including depression, panic and obsessive compulsive disorder, but was not beneficial in schizophrenia, dementia, Alzheimer's disease, attention deficit disorder, autism or electroconvulsive therapy-induced cognitive impairment (50).

Depression, an imbalance in mood-stabilization, is a common and important complication of primary cerebral glioma. The symptoms of depression may be a consequence of tumor, surgery, and/or adjuvant treatments. It has been reported that more than 30% of glioma patients have depression and that most glioma patients exhibit symptoms of depression after surgeries (26,27). In our study, the mood of tumor-bearing rats was evaluated. SAHA-treated rats bearing tumors showed improved mood-related behaviors compared to untreated rats, including signs of increased appetite, social interactions, and locomotive activities. Combined with the increased levels of NAA and Ins, the improved mood-related behaviors

observed in SAHA-treated rats may indicate that SAHA is effective in treating both high-grade gliomas and glioma-related depression.

In conclusion, we have established reliable metabolic biomarkers that predict therapeutic response at the earliest stage of SAHA treatment. After only 3 days of SAHA treatment, the concentrations of NAA, Cr, and Ins increased, and the concentrations of Lac and Ala decreased, as non-invasively measured by ^1H MRS. ISYNA1 mRNA levels from *in vivo* samples and *in vitro* samples confirmed dose-dependent responses to SAHA treatment. Mood-related behaviors in rats with brain tumors have been improved by SAHA treatment. Our results indicate that SAHA inhibits tumor growth and induces normal brain tissue-like metabolism in brain tumors. SAHA, as an HDAC inhibitor, is potentially an exciting anti-tumor agent for GBM treatment that induces redifferentiation, rather than cell-death. Establishing reliable MRS biomarkers as well as molecular pathological biomarker for assessing early response would clearly be of value in personalizing the management of GBM patients by aiding clinicians in adjusting the dose of SAHA treatment or switching to alternative treatment. Importantly, translation of our MRS-based tool will assess the restoration of normal brain metabolism, and indirectly monitors the subject's quality of life in the clinic.

Acknowledgments

This work was supported by NIH grants CA109366 (HS) and CA128301 (HS, JJO and XPH). This work was supported in part by the Biomedical Imaging Technology Center. We thank Ms. Jessica Paulishen for careful reading of the manuscript and helpful remarks. We thank Drs. Thaddeus Pace and Andrew Miller for their help on interpretation of depressive behavior. We thank NCI/CTEP for supplying preclinical batch of Vorinostat.

Abbreviations used

Ala	alanine
Asp	aspartate
BBB	blood brain barrier
Cho	choline
Cr	creatinine
DMSO	dimethyl sulfoxide
DQC	double quantum coherent
GABA	gamma-aminobutyrate
GBM	Glioblastoma
Glc	glucose
Gln	glutamine
Glu	glutamate
Gly	glycine
GPC	glycerophosphocholine
GSH	glutathione
Gua	guanidoacetate
HDAC	histone deacetylase
HDACi	histone deacetylase inhibitor

Ins	inositol
Lac	lactate
MQC	multiple quantum coherences
NAA(G)	N-acetylaspartate (glutamate)
pCho	phosphocholine
pCr	phosphocreatine
SAHA	Suberoylanilide hydroxamic acid
Sel-DQC	selective-DQC
sI	scyllo-Inositol
STEAM	stimulated-echo acquisition mode
Tau	taurine
tCho	total Cho
tCr	total Cr

REFERENCES

1. Stupp R, Mason WP, van den Bent MJ, Weller M, Fisher B, Taphoorn MJ, Belanger K, Brandes AA, Marosi C, Bogdahn U, Curschmann J, Janzer RC, Ludwin SK, Gorlia T, Allgeier A, Lacombe D, Cairncross JG, Eisenhauer E, Mirimanoff RO. Radiotherapy plus concomitant and adjuvant temozolomide for glioblastoma. *N Engl J Med*. 2005; 352(10):987–996. [PubMed: 15758009]
2. Scott AW, Tyler BM, Masi BC, Upadhyay UM, Patta YR, Grossman R, Basaldella L, Langer RS, Brem H, Cima MJ. Intracranial microcapsule drug delivery device for the treatment of an experimental gliosarcoma model. *Biomaterials*. 2011; 32(10):2532–2539. [PubMed: 21220172]
3. Tredan O, Galmarini CM, Patel K, Tannock IF. Drug resistance and the solid tumor microenvironment. *Journal of the National Cancer Institute*. 2007; 99(19):1441–1454. [PubMed: 17895480]
4. Nagarajan RP, Costello JF. Molecular epigenetics and genetics in neuro-oncology. *Neurotherapeutics*. 2009; 6(3):436–446. [PubMed: 19560734]
5. Nagarajan RP, Costello JF. Epigenetic mechanisms in glioblastoma multiforme. *Semin Cancer Biol*. 2009; 19(3):188–197. [PubMed: 19429483]
6. Natsume A, Kondo Y, Ito M, Motomura K, Wakabayashi T, Yoshida J. Epigenetic aberrations and therapeutic implications in gliomas. *Cancer Sci*. 2010; 101(6):1331–1336. [PubMed: 20384628]
7. Rundlett SE, Carmen AA, Suka N, Turner BM, Grunstein M. Transcriptional repression by UME6 involves deacetylation of lysine 5 of histone H4 by RPD3. *Nature*. 1998; 392(6678):831–835. [PubMed: 9572144]
8. Jones PA, Baylin SB. The fundamental role of epigenetic events in cancer. *Nature reviews Genetics*. 2002; 3(6):415–428.
9. Ellis L, Pili R. Histone Deacetylase Inhibitors: Advancing Therapeutic Strategies in Hematological and Solid Malignancies. *Pharmaceuticals (Basel)*. 2010; 3(8):2411–2469. [PubMed: 21151768]
10. Bumber Y, Issa JP. Epigenetics in cancer: what's the future? *Oncology (Williston Park)*. 2011; 25(3):220–226. 228. [PubMed: 21548464]
11. Piekarz RL, Robey RW, Zhan Z, Kayastha G, Sayah A, Abdeldaim AH, Torrico S, Bates SE. T-cell lymphoma as a model for the use of histone deacetylase inhibitors in cancer therapy: impact of depsiptide on molecular markers, therapeutic targets, and mechanisms of resistance. *Blood*. 2004; 103(12):4636–4643. [PubMed: 14996704]

12. Prince HM, Bishton MJ, Harrison SJ. Clinical studies of histone deacetylase inhibitors. *Clinical cancer research : an official journal of the American Association for Cancer Research*. 2009; 15(12):3958–3969. [PubMed: 19509172]
13. Fandy TE, Shankar S, Ross DD, Sausville E, Srivastava RK. Interactive effects of HDAC inhibitors and TRAIL on apoptosis are associated with changes in mitochondrial functions and expressions of cell cycle regulatory genes in multiple myeloma. *Neoplasia*. 2005; 7(7):646–657. [PubMed: 16026644]
14. Yin D, Ong JM, Hu J, Desmond JC, Kawamata N, Konda BM, Black KL, Koeffler HP. Suberoylanilide hydroxamic acid, a histone deacetylase inhibitor: effects on gene expression and growth of glioma cells in vitro and in vivo. *Clin Cancer Res*. 2007; 13(3):1045–1052. [PubMed: 17289901]
15. Rodriguez-Gonzalez A, Lin T, Ikeda AK, Simms-Waldrup T, Fu C, Sakamoto KM. Role of the aggresome pathway in cancer: targeting histone deacetylase 6-dependent protein degradation. *Cancer research*. 2008; 68(8):2557–2560. [PubMed: 18413721]
16. Komatsu N, Kawamata N, Takeuchi S, Yin D, Chien W, Miller CW, Koeffler HP. SAHA, a HDAC inhibitor, has profound anti-growth activity against non-small cell lung cancer cells. *Oncology reports*. 2006; 15(1):187–191. [PubMed: 16328054]
17. Cohen LA, Marks PA, Rifkind RA, Amin S, Desai D, Pittman B, Richon VM. Suberoylanilide hydroxamic acid (SAHA), a histone deacetylase inhibitor, suppresses the growth of carcinogen-induced mammary tumors. *Anticancer research*. 2002; 22(3):1497–1504. [PubMed: 12168829]
18. Hsi LC, Xi X, Lotan R, Shureiqi I, Lippman SM. The histone deacetylase inhibitor suberoylanilide hydroxamic acid induces apoptosis via induction of 15-lipoxygenase-1 in colorectal cancer cells. *Cancer research*. 2004; 64(23):8778–8781. [PubMed: 15574791]
19. Eyupoglu IY, Hahnen E, Buslei R, Siebzehnrubl FA, Savaskan NE, Luders M, Trankle C, Wick W, Weller M, Fahlbusch R, Blumcke I. Suberoylanilide hydroxamic acid(SAHA) has potent anti-glioma properties in vitro, ex vivo and in vivo. *J Neurochem*. 2005; 93(4):992–999. [PubMed: 15857402]
20. Li X, Jin H, Lu Y, Oh J, Chang S, Nelson SJ. Identification of MRI and 1H MRSI parameters that may predict survival for patients with malignant gliomas. *NMR in biomedicine*. 2004; 17(1):10–20. [PubMed: 15011246]
21. Oh J, Henry RG, Pirzkall A, Lu Y, Li X, Catalaa I, Chang S, Dillon WP, Nelson SJ. Survival analysis in patients with glioblastoma multiforme: predictive value of cholineto-N-acetylaspartate index, apparent diffusion coefficient, and relative cerebral blood volume. *Journal of magnetic resonance imaging : JMRI*. 2004; 19(5):546–554. [PubMed: 15112303]
22. Salway, JG. *Metabolism at a glance*. Malden, Mass.: Blackwell Pub.; 2004. p. 125
23. Lehninger, AL.; Nelson, DL.; M, CM. *Lehninger principles of biochemistry*. 4, editor. New York: W.H Freeman; 2005.
24. Castillo M, Smith JK, Kwock L. Correlation of myo-inositol levels and grading of cerebral astrocytomas. *AJNR Am J Neuroradiol*. 2000; 21(9):1645–1649. [PubMed: 11039343]
25. Hattingen E, Raab P, Franz K, Zanella FE, Lanfermann H, Pilatus U. Myo-inositol: a marker of reactive astrogliosis in glial tumors? *NMR in biomedicine*. 2008; 21(3):233–241. [PubMed: 17562554]
26. Talacchi A, Santini B, Savazzi S, Gerosa M. Cognitive effects of tumour and surgical treatment in glioma patients. *Journal of neuro-oncology*. 2010
27. Rooney AG, Carson A, Grant R. Depression in cerebral glioma patients: a systematic review of observational studies. *Journal of the National Cancer Institute*. 2011; 103(1):61–76. [PubMed: 21106962]
28. Kang SH, Cho HT, Devi S, Zhang Z, Escuin D, Liang Z, Mao H, Brat DJ, Olson JJ, Simons JW, Lavallee TM, Giannakakou P, Van Meir EG, Shim H. Antitumor effect of 2-methoxyestradiol in a rat orthotopic brain tumor model. *Cancer Res*. 2006; 66(24):11991–11997. [PubMed: 17178898]
29. Allen PS, Thompson RB, Wilman AH. Metabolite-specific NMR spectroscopy in vivo. *NMR Biomed*. 1997; 10(8):435–444. [PubMed: 9542740]
30. Zhao T, Heberlein K, Jonas C, Jones DP, Hu X. New double quantum coherence filter for localized detection of glutathione in vivo. *Magn Reson Med*. 2006; 55(3):676–680. [PubMed: 16447170]

31. Bradner JE, West N, Grachan ML, Greenberg EF, Haggarty SJ, Warnow T, Mazitschek R. Chemical phylogenetics of histone deacetylases. *Nat Chem Biol.* 2010; 6(3):238–243. [PubMed: 20139990]
32. Ugur HC, Ramakrishna N, Bello L, Menon LG, Kim SK, Black PM, Carroll RS. Continuous intracranial administration of suberoylanilide hydroxamic acid (SAHA) inhibits tumor growth in an orthotopic glioma model. *J Neurooncol.* 2007; 83(3):267–275. [PubMed: 17310267]
33. Galanis E, Jaeckle KA, Maurer MJ, Reid JM, Ames MM, Hardwick JS, Reilly JF, Loboda A, Nebozhyn M, Fantin VR, Richon VM, Scheithauer B, Giannini C, Flynn PJ, Moore DF Jr, Zwiebel J, Buckner JC. Phase II trial of vorinostat in recurrent glioblastoma multiforme: a north central cancer treatment group study. *J Clin Oncol.* 2009; 27(12):2052–2058. [PubMed: 19307505]
34. Panigrahy A, Bluml S. Neuroimaging of pediatric brain tumors: from basic to advanced magnetic resonance imaging (MRI). *Journal of child neurology.* 2009; 24(11):1343–1365. [PubMed: 19841424]
35. Kelly WK, Richon VM, O'Connor O, Curley T, MacGregor-Curtelli B, Tong W, Klang M, Schwartz L, Richardson S, Rosa E, Drobnjak M, Cordon-Cordo C, Chiao JH, Rifkind R, Marks PA, Scher H. Phase I clinical trial of histone deacetylase inhibitor: suberoylanilide hydroxamic acid administered intravenously. *Clinical cancer research : an official journal of the American Association for Cancer Research.* 2003; 9(10 Pt 1):3578–3588. [PubMed: 14506144]
36. Opstad KS, Ladroue C, Bell BA, Griffiths JR, Howe FA. Linear discriminant analysis of brain tumour (1)H MR spectra: a comparison of classification using whole spectra versus metabolite quantification. *NMR in biomedicine.* 2007; 20(8):763–770. [PubMed: 17326043]
37. Weis J, Ring P, Olofsson T, Ortiz-Nieto F, Wikstrom J. Short echo time MR spectroscopy of brain tumors: grading of cerebral gliomas by correlation analysis of normalized spectral amplitudes. *Journal of magnetic resonance imaging : JMRI.* 2010; 31(1):39–45. [PubMed: 20027571]
38. Preul MC, Leblanc R, Caramanos Z, Kasrai R, Narayanan S, Arnold DL. Magnetic resonance spectroscopy guided brain tumor resection: differentiation between recurrent glioma and radiation change in two diagnostically difficult cases. *The Canadian journal of neurological sciences Le journal canadien des sciences neurologiques.* 1998; 25(1):13–22. [PubMed: 9532276]
39. Lai PH, Weng HH, Chen CY, Hsu SS, Ding S, Ko CW, Fu JH, Liang HL, Chen KH. In vivo differentiation of aerobic brain abscesses and necrotic glioblastomas multiforme using proton MR spectroscopic imaging. *AJNR Am J Neuroradiol.* 2008; 29(8):1511–1518. [PubMed: 18499784]
40. Sankar T, Caramanos Z, Assina R, Villemure JG, Leblanc R, Langleben A, Arnold DL, Preul MC. Prospective serial proton MR spectroscopic assessment of response to tamoxifen for recurrent malignant glioma. *Journal of neuro-oncology.* 2008; 90(1):63–76. [PubMed: 18600428]
41. Howe FA, Barton SJ, Cudlip SA, Stubbs M, Saunders DE, Murphy M, Wilkins P, Opstad KS, Doyle VL, McLean MA, Bell BA, Griffiths JR. Metabolic profiles of human brain tumors using quantitative in vivo 1H magnetic resonance spectroscopy. *Magnetic resonance in medicine : official journal of the Society of Magnetic Resonance in Medicine / Society of Magnetic Resonance in Medicine.* 2003; 49(2):223–232. [PubMed: 12541241]
42. Barker PB. N-acetyl aspartate--a neuronal marker? *Annals of neurology.* 2001; 49(4):423–424. [PubMed: 11310618]
43. Tzika AA, Zurakowski D, Poussaint TY, Goumnerova L, Astrakas LG, Barnes PD, Anthony DC, Billett AL, Tarbell NJ, Scott RM, Black PM. Proton magnetic spectroscopic imaging of the child's brain: the response of tumors to treatment. *Neuroradiology.* 2001; 43(2):169–177. [PubMed: 11326567]
44. Semenza GL. Tumor metabolism: cancer cells give and take lactate. *The Journal of clinical investigation.* 2008; 118(12):3835–3837. [PubMed: 19033652]
45. Munster PN, Troso-Sandoval T, Rosen N, Rifkind R, Marks PA, Richon VM. The histone deacetylase inhibitor suberoylanilide hydroxamic acid induces differentiation of human breast cancer cells. *Cancer research.* 2001; 61(23):8492–8497. [PubMed: 11731433]
46. Covington HE 3rd, Maze I, LaPlant QC, Vialou VF, Ohnishi YN, Berton O, Fass DM, Renthall W, Rush AJ 3rd, Wu EY, Ghose S, Krishnan V, Russo SJ, Tamminga C, Haggarty SJ, Nestler EJ. Antidepressant actions of histone deacetylase inhibitors. *J Neurosci.* 2009; 29(37):11451–11460. [PubMed: 19759294]

47. Baraban JM, Worley PF, Snyder SH. Second messenger systems and psychoactive drug action: focus on the phosphoinositide system and lithium. *The American journal of psychiatry*. 1989; 146(10):1251–1260. [PubMed: 2571304]
48. Barkai AI. Dopamine turnover in the intact rabbit brain: effect of pentobarbital or haloperidol. *J Pharmacol Exp Ther*. 1978; 205(1):133–140. [PubMed: 633078]
49. Levine J, Rapaport A, Lev L, Bersudsky Y, Kofman O, Belmaker RH, Shapiro J, Agam G. Inositol treatment raises CSF inositol levels. *Brain research*. 1993; 627(1):168–170. [PubMed: 8293297]
50. Levine J. Controlled trials of inositol in psychiatry. *European Neuropsychopharmacology*. 1997; 7(2):147–155. [PubMed: 9169302]

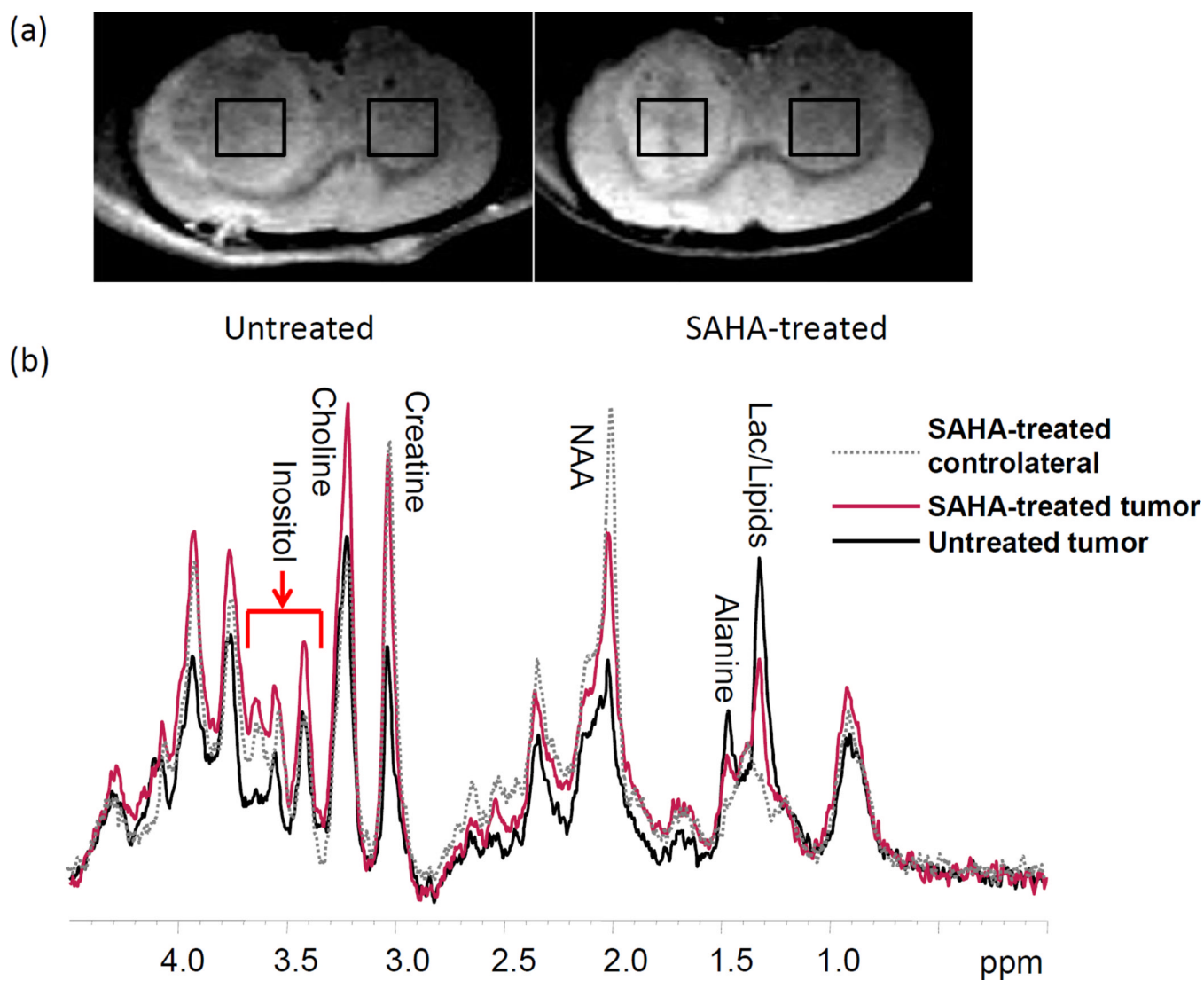


Figure 1.

(a) T₂-weighted images of untreated (Left) and SAHA-treated (Right) rats, on which representative regions of interesting used for MR spectroscopy are shown (TR/TE=2500/45 ms). (b) *In vivo* ¹H MRS (STEAM) obtained from the tumor side with (red) and without (black) SAHA treatment. The grey dotted line was that obtained from SAHA-treated contralateral side (non-tumor side).

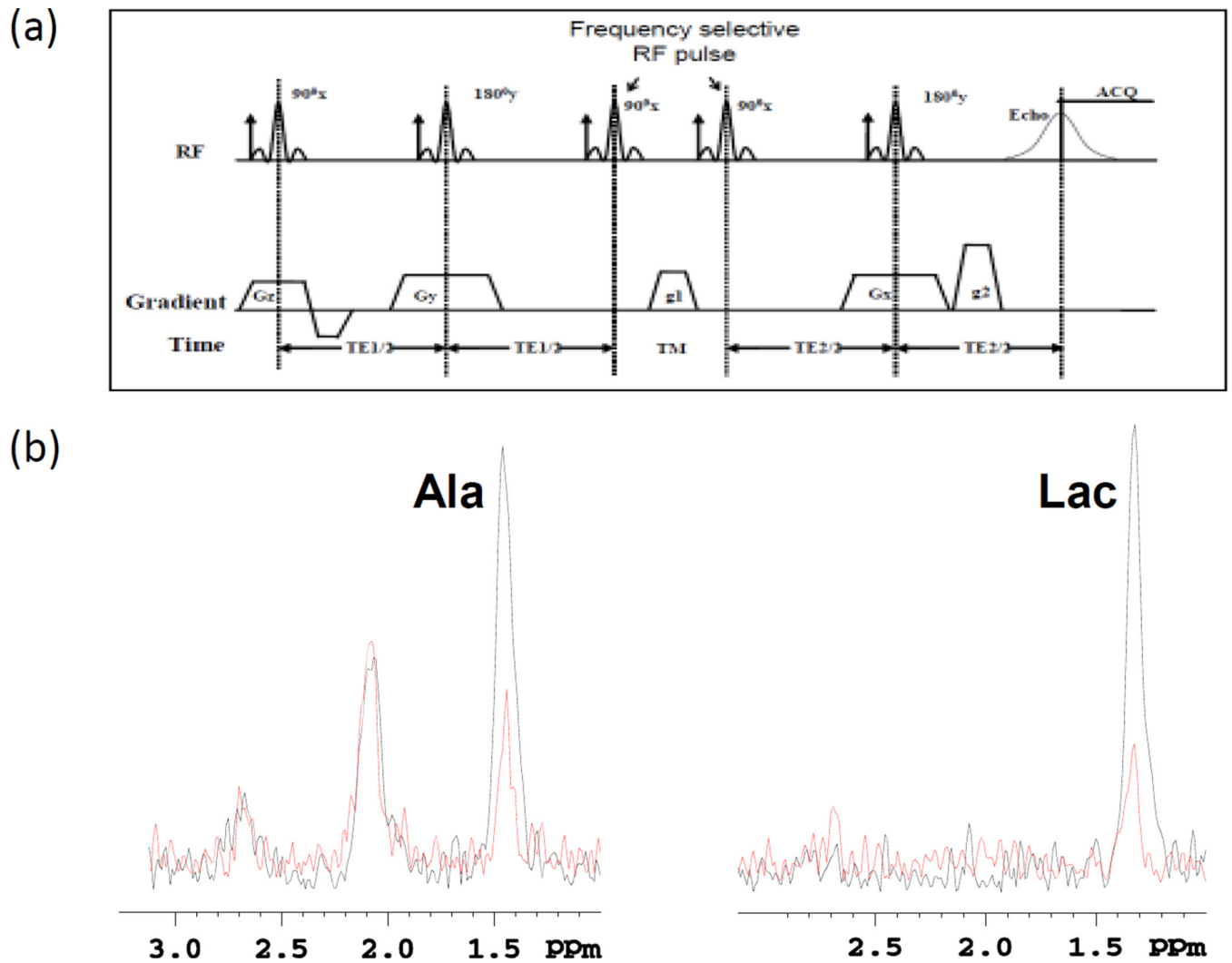


Figure 2.
 (a) Frequency-Selective Double Quantum Coherence (Sel-DQC) sequence for Ala and Lac detection. (b) *In vivo* ^1H Sel-DQC spectrum of Ala and Lac obtained from the tumors with (red) and without (black) SAHA treatment (TR/TE/TM=3000/70/14 ms).

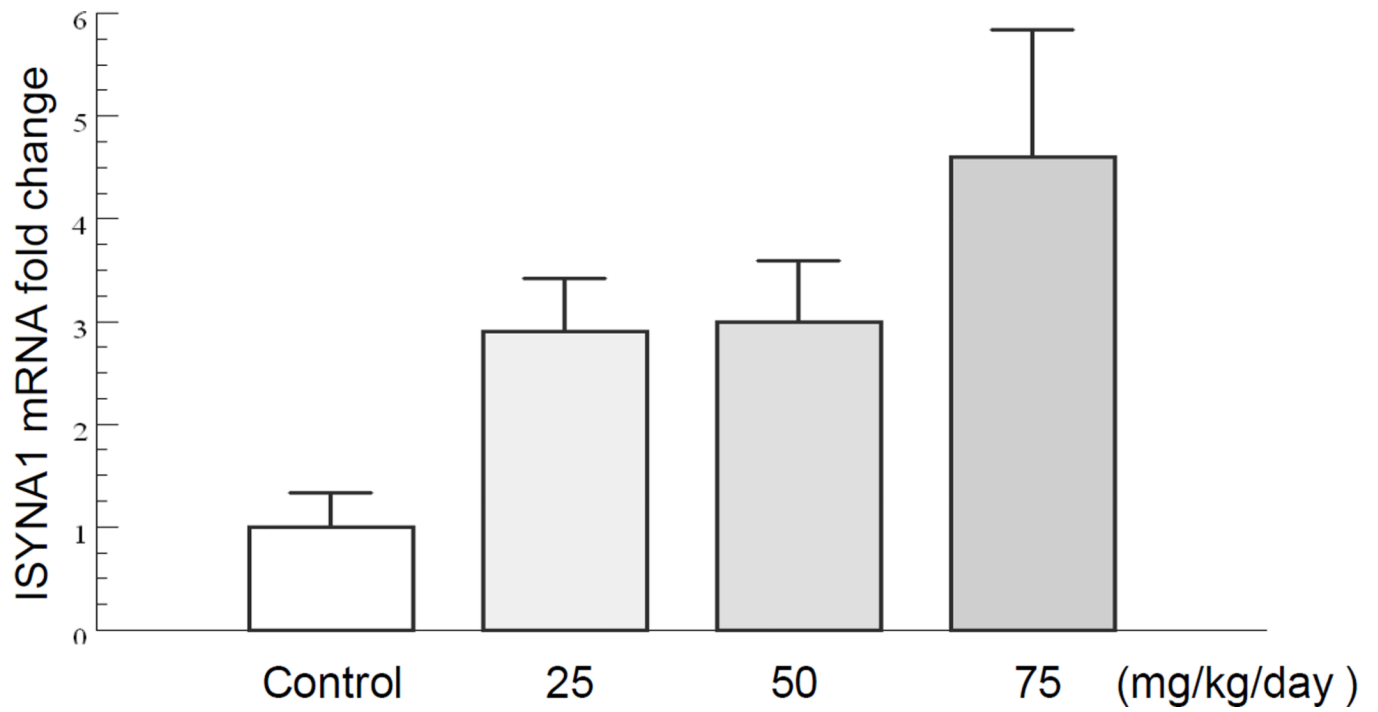


Figure 3. Dose-dependent relative fold-change of ISYNA1 mRNA level in tumors from SAHA-treated group and untreated (vehicle) group.

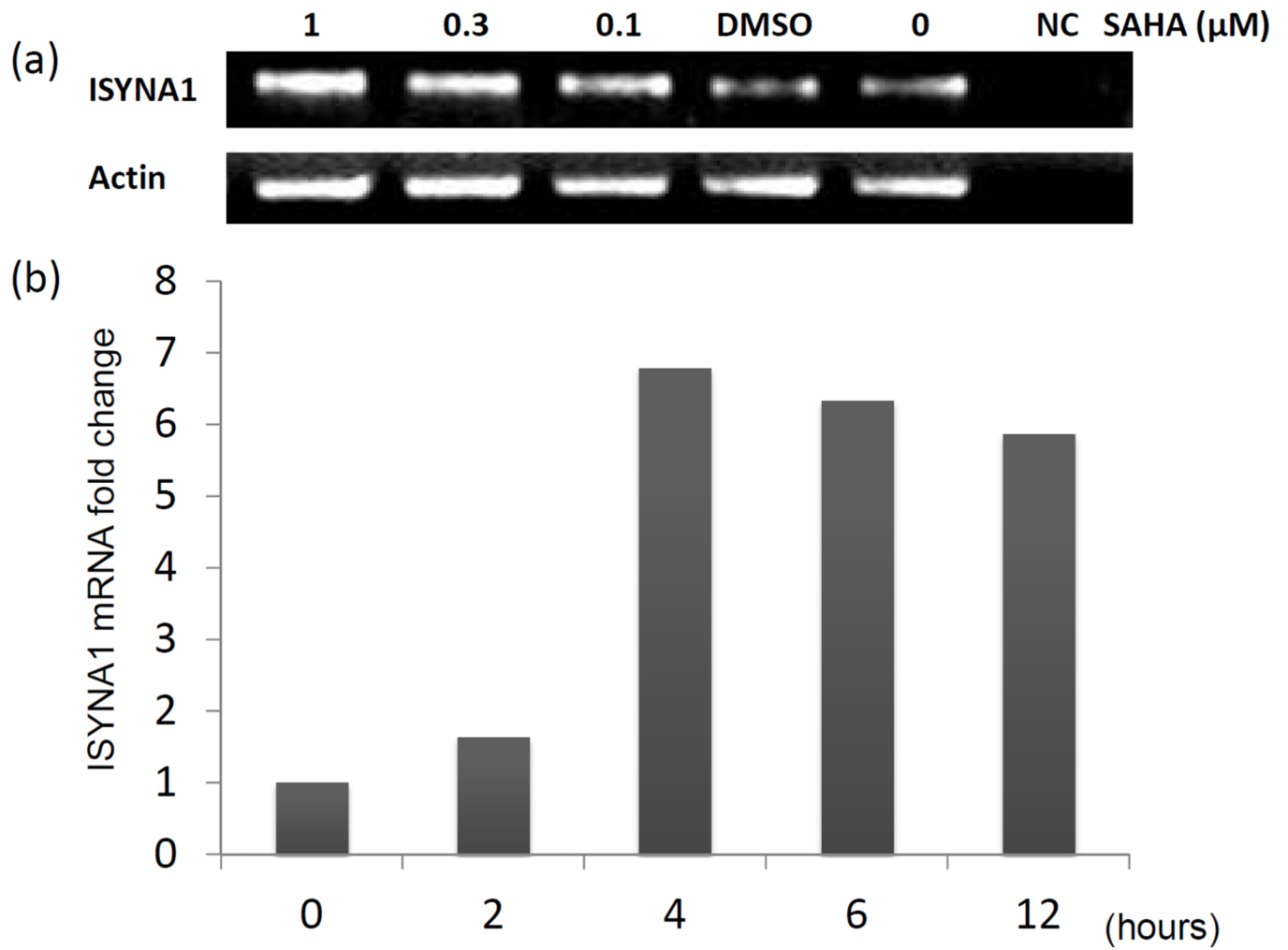


Figure 4. (a) ISYNA1 mRNA level in 9L cells with different doses of SAHA administration. (b) Time-dependent relative fold-change of ISYNA1 mRNA level in 9L cells after administering 1 μM of SAHA.

Table 1Metabolite concentrations (mM) shown in mean \pm s.d.

Metabolites	Cho	NAA+NAAG	Cr	Ins	Lac	Ala
SAHA_contralateral (N=8)	1.42 \pm 0.67	9.34 \pm 0.49	11.25 \pm 0.7	6.36 \pm 0.72	1.39 \pm 0.73	0.2 \pm 0.16
SAHA_tumor	2.34 \pm 1.01	5.47 \pm 0.8*	9.07 \pm 0.85**	5.58 \pm 0.95*	3.45 \pm 0.81**	1.26 \pm 0.54**
Untreated_contralateral (N=6)	1.24 \pm 0.74	7.89 \pm 0.59	9.92 \pm 0.7	5.54 \pm 0.73	1.16 \pm 0.33	0.17 \pm 0.16
Untreated_tumor	2.28 \pm 1.43	2.38 \pm 1.14	4.96 \pm 2.02	3.80 \pm 0.37	6.05 \pm 2.22	3.48 \pm 0.85

Statistical analysis was performed with student *t*-tests.

* p<0.05 compared with Untreated_tumor,

** p<0.01 compared with Untreated_tumor